2023 62nd IEEE Conference on Decision and Control (CDC)
December 13-15, 2023. Marina Bay Sands, Singapore

Optimization-Based Bound Tightening using a Strengthened QC-Relaxation of the Optimal Power Flow Problem

Kaarthik Sundar, Harsha Nagarajan, Sidhant Misra, Mowen Lu, Carleton Coffrin, and Russell Bent

***Abstract*— This paper develops a novel strengthened convex quadratic convex (QC) relaxation of the AC Optimal Power Flow (AC-OPF) problem and presents an optimization-based bound-tightening (OBBT) algorithm to compute tight, feasible bounds on the voltage magnitude variables for each bus and the phase angle difference variables for each branch in the network. Theoretical properties of the strengthened QC relaxation, that show its dominance over the other variants of the QC relaxation studied in the literature, are also derived. The effectiveness of the strengthened QC relaxation is corroborated via extensive numerical results on benchmark AC-OPF test networks. In particular, the results demonstrate that the proposed relaxation consistently provides the tightest variable bounds and optimality gaps with negligible impacts on runtime performance.**

I. Introduction

The AC Optimal Power Flow (AC-OPF) problem is one of the most fundamental optimization problems for economic and reliable operation of the electric transmission system. Since its introduction in 1962 [1], efficient solution techniques to solve the AC-OPF have garnered a lot of attention from the research community. The objective of the AC-OPF is to minimize the generation cost while satisfying the power flow constraints and the network limits. The fundamental difficultly with solving the AC-OPF arises due to the non-linear and non-convex nature of the power flow constraints. The literature with regards to AC-OPF can predominantly be classified into the one of the following three groups: (i) developing fast algorithms to compute a local optimal solution to the AC-OPF either using meta-heuristics or numeral techniques like gradient descent [2] etc., (ii) developing convex relaxations that convexify the feasible space defined by the AC-OPF, and (iii) developing global optimization algorithms for AC-OPF [3], [4]. The NP-hardness of AC-OPF [5] makes guarantees on feasibility and global optimality very difficult and hence, the past decade has seen a surge in the work devoted towards developing convex relaxations of AC-OPF. They include the Semi-Definite Programming (SDP) [6], Second Order Cone (SOC) [7], the recent Quadratic Convex (QC) [8] and Moment-Based [9] relaxations. In general, convex relaxations of AC-OPF are appealing because they can provide lower bounds to the AC-OPF objective value, prove infeasibility of the AC-OPF, or can aid in proving global optimality by producing a feasible solution in the non-convex space defined by the AC-OPF. One major factor that parameterizes the strength of the convex relaxation for the AC-OPF is the variable bounds. This dependence goes both ways, i.e., tightened bounds can aid in providing tighter convex relaxations and better convex relaxations can aid in tightening the variable bounds even further [10], [11]. In this paper, we exploit this dependence between bound-tightening and strong convex relaxations in two novel ways: (i) we first present a strengthened QC relaxation that uses an extreme-point representation and strictly dominates the state-of-the-art QC relaxations in the literature [4], [8] and (ii) we develop an optimality-based bound-tightening algorithm (OBBT) that exploits the strengthened QC relaxations. These two novel contributions are put together to obtain lower bounds, that are better than the current known lower bounds, for the benchmark AC-OPF problem instances. We also note that variants of the bound-tightening algorithm presented in this paper are used routinely in the mixed-integer nonlinear programming literature [12], [13] and also in algorithmic approaches used to tighten variable bounds in AC-OPF [10], [14]. Furthermore, we show useful theoretical properties of the strengthened QC relaxation, which also have a potential to generalize to other variants of the AC-OPF relaxations, such as in the inclusion of polynomial cycle constraints [3]. Finally, we present extensive experimental results that demonstrate the value of the convex relaxation applied in conjunction with OBBT. In particular, we show that

1) The strengthened QC relaxation is able to obtain the tightest voltage and phase angle difference bounds for the AC-OPF problem compared to the other QC relaxations in the literature.
2) When utilized in the context of global optimization of AC-OPF with OBBT, on networks with less than 1000 buses, the strengthened QC relaxation results in an optimality gap of $< 1\%$ for 52 out of 57 networks.

Nomenclature

Sets and Parameters

$\mathcal{N}$ - set of nodes (buses)
$\mathcal{G}$ - set of generators
$\mathcal{G}_i$ - set of generators at bus i
$\mathcal{E}$ - set of *from* edges (branches)
$\mathcal{E}^{\mathcal{R}}$ - set of *to* edges (branches)
$\boldsymbol{c_0}, \boldsymbol{c_1}, \boldsymbol{c_2}$ - generation cost coefficients
$\boldsymbol{i}$ - imaginary number constant
$\boldsymbol{Z_{ij}} = \boldsymbol{r_{ij}} + \boldsymbol{ix_{ij}}$ - impedance on branch ij
$\boldsymbol{Y_{ij}} = \boldsymbol{g_{ij}} + \boldsymbol{ib_{ij}}$ - admittance on branch ij
$\boldsymbol{S_i^d} = \boldsymbol{p_i^d} + \boldsymbol{iq_i^d}$ - Aggregated AC power demand at bus i
$\boldsymbol{s_{ij}^u}$ - apparent power limit on branch ij
$\boldsymbol{\theta_{ij}^l}, \boldsymbol{\theta_{ij}^u}$ - phase angle difference limits on branch ij

K. Sundar, H. Nagarajan, S. Misra, C. Coffrin and R. Bent are with Los Alamos National Laboratory, Los Alamos, NM, USA (Contacts: {kaarthik, harsha, sidhant, cjc, rbent}@lanl.gov).

M. Lu is with Walmart Global Tech, Sunnyvale, CA, USA.

Model 1 AC Optimal Power Flow (AC-OPF) problem

$$\textbf{minimize:} \quad \sum_{i\in\mathcal{G}} \boldsymbol{c}_{2i}(\Re(S_i^g)^2) + \boldsymbol{c}_{1i}\Re(S_i^g) + \boldsymbol{c}_{0i} \tag{1a}$$

subject to:

$$\sum_{k\in\mathcal{G}_i} S_k^g - \boldsymbol{S_i^d} = \sum_{(i,j)\in\mathcal{E}\cup\mathcal{E}^{\mathcal{R}}} S_{ij} \quad \forall i \in \mathcal{N} \tag{1b}$$

$$S_{ij} = \boldsymbol{Y}_{ij}^* W_{ii} - \boldsymbol{Y}_{ij}^* W_{ij} \quad \forall (i,j) \in \mathcal{E} \tag{1c}$$

$$S_{ji} = \boldsymbol{Y}_{ij}^* W_{jj} - \boldsymbol{Y}_{ij}^* W_{ij}^* \quad \forall (i,j) \in \mathcal{E} \tag{1d}$$

$$W_{ii} = |V_i|^2 \quad \forall i \in \mathcal{N} \tag{1e}$$

$$W_{ij} = V_i V_j^* \quad \forall (i,j) \in \mathcal{E} \tag{1f}$$

$$\boldsymbol{\theta_{ij}^l} \leqslant \theta_{ij} \leqslant \boldsymbol{\theta_{ij}^u} \quad \forall (i,j) \in \mathcal{E} \tag{1g}$$

$$(\boldsymbol{v_i^l})^2 \leqslant W_{ii} \leqslant (\boldsymbol{v_i^u})^2 \quad \forall i \in \mathcal{N} \tag{1h}$$

$$\boldsymbol{S_i^{gl}} \leqslant S_i^g \leqslant \boldsymbol{S_i^{gu}} \quad \forall i \in \mathcal{G} \tag{1i}$$

$$|S_{ij}| \leqslant \boldsymbol{s_{ij}^u} \quad \forall (i,j) \in \mathcal{E} \cup \mathcal{E}^{\mathcal{R}} \tag{1j}$$

$\boldsymbol{\theta_{ij}^m}$ - $\max(|\boldsymbol{\theta_{ij}^l}|, |\boldsymbol{\theta_{ij}^u}|)$ on branch ij
$\boldsymbol{v_i^l}, \boldsymbol{v_i^u}$ - voltage magnitude limit at bus i
$\boldsymbol{S_i^{gl}}$, $\boldsymbol{S_i^{gu}}$ - power generation limit at bus i
$\Re(\cdot)$ - real part of a complex number
$\Im(\cdot)$ - imaginary part of a complex number
$(\cdot)^*$ - hermitian conjugate of a complex number
$|\cdot|, \angle\cdot$ - magnitude, angle of a complex number

Continuous variables
$V_i = v_i \boldsymbol{e}^{\boldsymbol{i}\theta_i}$ - AC voltage at bus i
$\theta_{ij} = \angle V_i - \angle V_j$ - phase angle difference on branch ij
W_{ij} - AC voltage product on branch ij, i.e., $V_i V_j^*$
$S_{ij} = p_{ij} + \boldsymbol{i} q_{ij}$ - AC power flow on branch ij
$S_i^g = p_i^g + \boldsymbol{i} q_i^g$ - AC power generation at bus i
l_{ij} - current magnitude squared on branch ij

Notation In this paper, constants are typeset in bold face. In the AC power flow equations, the primitives, V_i, S_{ij}, S_i^g, $\boldsymbol{S_i^d}$ and $\boldsymbol{Y}_{ij}$ are complex quantities. Given any two complex numbers (variables/constants) z_1 and z_2, $z_1 \geqslant z_2$ implies $\Re(z_1) \geqslant \Re(z_2)$ and $\Im(z_1) \geqslant \Im(z_2)$. $|\cdot|$ represents absolute value when applied to a real number.

II. The Strengthened QC Relaxation

This section presents an overview of the mathematical formulation of the AC-OPF and its state-of-the-art QC relaxation and develops the strengthened QC relaxation for the AC-OPF.

A. AC Optimal Power Flow

We start by presenting the mathematical formulation of the AC-OPF problem in Model 1 with additional W_{ij} and W_{ii} variables for each branch and bus, respectively. The optimal solution to the AC-OPF problem minimizes generation costs for a specified demand and satisfies engineering constraints and power flow physics.

The convex quadratic objective (1a) minimizes total generation cost. Constraint (1b) enforces nodal power balance at each bus. Constraints (1c) through (1f) model the AC power flow on each branch. Constraint (1g) limits the phase angle difference on each branch. Constraint (1h) limits the voltage magnitude square at each bus. Constraint (1i) restricts the apparent power output of each generator. Finally, constraint (1j) restricts the apparent power transmitted on each branch. For simplicity, we omit the details of constant bus shunt injections, transformer taps, phase shifts, and line charging, though we include them in the computational studies. The AC-OPF is a hard, non-convex problem [15], with non-convexities arising from the constraints (1e) and (1f).

B. QC Relaxation using Recursive McCormick Envelopes

The quadratic convex relaxation of the AC-OPF, proposed in [8], [16], is inspired by an arithmetic analysis of (1e) and (1f) in polar coordinates (i.e., $V_i = v_i \angle\theta_i \ \forall i \in \mathcal{N}$) with the goal of preserving stronger links between the voltage variables. Rewriting Eq. (1e) and (1f) using the polar voltage variables, the non-convexities reduce to the following equations:

$$W_{ii} = v_i^2 \quad \forall i \in \mathcal{N} \tag{2a}$$

$$\Re(W_{ij}) = v_i v_j \cos(\theta_{ij}) \quad \forall (i,j) \in \mathcal{E} \tag{2b}$$

$$\Im(W_{ij}) = v_i v_j \sin(\theta_{ij}) \quad \forall (i,j) \in \mathcal{E} \tag{2c}$$

Each of the above non-convex equations are then relaxed by composing convex envelopes of the non-convex sub-expressions using the bounds on v_i, v_j, θ_{ij} variables. For the square and product of variables, the QC relaxation uses the well-known McCormick envelopes [17], given by (T-CONV) and (M-CONV), respectively, as follows:

$$\langle x^2 \rangle^T \equiv \begin{cases} \breve{x} \geqslant x^2 \\ \breve{x} \leqslant (\boldsymbol{x^u} + \boldsymbol{x^l})x - \boldsymbol{x^u x^l} \end{cases} \tag{T-CONV}$$

$$\langle xy \rangle^M \equiv \begin{cases} \breve{xy} \geqslant \boldsymbol{x^l} y + \boldsymbol{y^l} x - \boldsymbol{x^l y^l} \\ \breve{xy} \geqslant \boldsymbol{x^u} y + \boldsymbol{y^u} x - \boldsymbol{x^u y^u} \\ \breve{xy} \leqslant \boldsymbol{x^l} y + \boldsymbol{y^u} x - \boldsymbol{x^l y^u} \\ \breve{xy} \leqslant \boldsymbol{x^u} y + \boldsymbol{y^l} x - \boldsymbol{x^u y^l} \end{cases} \tag{M-CONV}$$

The above convex envelopes are parameterized by the variable bounds (i.e., $\boldsymbol{x^l}, \boldsymbol{x^u}, \boldsymbol{y^l}, \boldsymbol{y^u}$). The convex envelopes for the cosine (C-CONV) and sine (S-CONV) functions, under the assumption that the phase angle difference bound satisfies $-\boldsymbol{\pi}/2 \leqslant \boldsymbol{\theta_{ij}^l} \leqslant \boldsymbol{\theta_{ij}^u} \leqslant \boldsymbol{\pi}/2$ [18], are given by

$$\langle \cos(x) \rangle^C \equiv \begin{cases} \breve{cs} \leqslant 1 - \frac{1-\cos(\boldsymbol{x^m})}{(\boldsymbol{x^m})^2} x^2 \\ \breve{cs} \geqslant \frac{\cos(\boldsymbol{x^l}) - \cos(\boldsymbol{x^u})}{(\boldsymbol{x^l} - \boldsymbol{x^u})} (x - \boldsymbol{x^l}) + \cos(\boldsymbol{x^l}) \end{cases}$$

$$\langle \sin(x) \rangle^S \equiv \begin{cases} \breve{sn} \leqslant \cos\left(\frac{\boldsymbol{x^m}}{2}\right)\left(x - \frac{\boldsymbol{x^m}}{2}\right) + \sin\left(\frac{\boldsymbol{x^m}}{2}\right) \\ \breve{sn} \geqslant \cos\left(\frac{\boldsymbol{x^m}}{2}\right)\left(x + \frac{\boldsymbol{x^m}}{2}\right) - \sin\left(\frac{\boldsymbol{x^m}}{2}\right) \\ \breve{sn} \geqslant \frac{\sin(\boldsymbol{x^l}) - \sin(\boldsymbol{x^u})}{(\boldsymbol{x^l} - \boldsymbol{x^u})}(x - \boldsymbol{x^l}) + \sin(\boldsymbol{x^l}) \text{ if } \boldsymbol{x^l} \geqslant 0 \\ \breve{sn} \leqslant \frac{\sin(\boldsymbol{x^l}) - \sin(\boldsymbol{x^u})}{(\boldsymbol{x^l} - \boldsymbol{x^u})}(x - \boldsymbol{x^l}) + \sin(\boldsymbol{x^l}) \text{ if } \boldsymbol{x^u} \leqslant 0 \end{cases}$$

Model 2 Original QC Relaxation (QC-RM).

$$\textbf{minimize:} \quad \sum_{i\in\mathcal{G}} \boldsymbol{c}_{2i}(\Re(S_i^g)^2) + \boldsymbol{c}_{1i}\Re(S_i^g) + \boldsymbol{c}_{0i} \tag{3a}$$

subject to: (1b) – (1d), (1g) – (1j), (5a) – (5b)

$$W_{ii} = \langle v_i^2 \rangle^T \quad i \in \mathcal{N} \tag{3b}$$

$$\Re(W_{ij}) = \langle \langle v_i v_j \rangle^M \langle \cos(\theta_{ij}) \rangle^C \rangle^M \quad \forall (i,j) \in \mathcal{E} \tag{3c}$$

$$\Im(W_{ij}) = \langle \langle v_i v_j \rangle^M \langle \sin(\theta_{ij}) \rangle^S \rangle^M \quad \forall (i,j) \in \mathcal{E} \tag{3d}$$

$$S_{ij} + S_{ji} = \boldsymbol{Z}_{ij} l_{ij} \quad \forall (i,j) \in \mathcal{E} \tag{3e}$$

$$|S_{ij}|^2 \leqslant W_{ii} l_{ij} \quad \forall (i,j) \in \mathcal{E} \tag{3f}$$

$$\forall (i,j) \in \mathcal{E}$$

$$\boldsymbol{v}_i^{\boldsymbol{\sigma}} \boldsymbol{v}_j^{\boldsymbol{\sigma}} (w_{ij}^R \cos(\boldsymbol{\phi}_{ij}) + w_{ij}^I \sin(\boldsymbol{\phi}_{ij})) - \boldsymbol{v}_j^{\boldsymbol{u}} \cos(\boldsymbol{\delta}_{ij}) \boldsymbol{v}_j^{\boldsymbol{\sigma}} w_i - \boldsymbol{v}_i^{\boldsymbol{u}} \cos(\boldsymbol{\delta}_{ij}) \boldsymbol{v}_i^{\boldsymbol{\sigma}} w_j \geqslant \boldsymbol{v}_i^{\boldsymbol{u}} \boldsymbol{v}_j^{\boldsymbol{u}} \cos(\boldsymbol{\delta}_{ij}) (\boldsymbol{v}_i^{\boldsymbol{l}} \boldsymbol{v}_j^{\boldsymbol{l}} - \boldsymbol{v}_i^{\boldsymbol{u}} \boldsymbol{v}_j^{\boldsymbol{u}}) \tag{5a}$$

$$\boldsymbol{v}_i^{\boldsymbol{\sigma}} \boldsymbol{v}_j^{\boldsymbol{\sigma}} (w_{ij}^R \cos(\boldsymbol{\phi}_{ij}) + w_{ij}^I \sin(\boldsymbol{\phi}_{ij})) - \boldsymbol{v}_j^{\boldsymbol{l}} \cos(\boldsymbol{\delta}_{ij}) \boldsymbol{v}_j^{\boldsymbol{\sigma}} w_i - \boldsymbol{v}_i^{\boldsymbol{l}} \cos(\boldsymbol{\delta}_{ij}) \boldsymbol{v}_i^{\boldsymbol{\sigma}} w_j \geqslant \boldsymbol{v}_i^{\boldsymbol{l}} \boldsymbol{v}_j^{\boldsymbol{l}} \cos(\boldsymbol{\delta}_{ij}) (\boldsymbol{v}_i^{\boldsymbol{u}} \boldsymbol{v}_j^{\boldsymbol{u}} - \boldsymbol{v}_i^{\boldsymbol{l}} \boldsymbol{v}_j^{\boldsymbol{l}}) \tag{5b}$$

respectively, where $\boldsymbol{x^m} = \max(|\boldsymbol{x^l}|, |\boldsymbol{x^u}|)$. The QC relaxation of the equations (2) is now obtained composing the convex envelopes for square, sine, cosine, and the product of two variables; the complete relaxation is shown in Model 2. In Model 2 and the models that follow, we abuse notation and let $\langle f(\cdot) \rangle^C$ denote the variable on the left-hand side of the convex envelope, C, for the function $f(\cdot)$. When such an expression is used inside an equation, the constraints $\langle f(\cdot) \rangle^C$ are also added to the model. Eq. (3e) and (3f) in Model 2 are convex constraints that connect apparent power flow on branches (S_{ij}) with current magnitude squared variables (l_{ij}). It is important to highlight that Model 2 includes the "Lifted Nonlinear Cuts" (LNCs) of [18], which further improve the version presented in [8], [16]. The LNCs are formulated using the following constants that are based on variable bounds, i.e.:

$$\boldsymbol{v}_i^{\boldsymbol{\sigma}} = \boldsymbol{v}_i^{\boldsymbol{l}} + \boldsymbol{v}_i^{\boldsymbol{u}} \quad \forall i \in \mathcal{N} \tag{4a}$$

$$\boldsymbol{\phi}_{ij} = (\boldsymbol{\theta}_{ij}^{\boldsymbol{u}} + \boldsymbol{\theta}_{ij}^{\boldsymbol{l}})/2 \quad \forall (i,j) \in \mathcal{E} \tag{4b}$$

$$\boldsymbol{\delta}_{ij} = (\boldsymbol{\theta}_{ij}^{\boldsymbol{u}} - \boldsymbol{\theta}_{ij}^{\boldsymbol{l}})/2 \quad \forall (i,j) \in \mathcal{E}. \tag{4c}$$

The LNCs are then given by (5a)-(5b), and are linear in the $w_i := W_{ii}, w_j := W_{jj}, w_{ij}^R := \Re(W_{ij}), w_{ij}^I := \Im(W_{ij})$ variables.

C. QC Relaxation using Extreme Point Representation

We now present an alternate QC relaxation that uses an extreme-point representation, instead of applying the McCormick constraints recursively, to express the convex envelope of $\Re(W_{ij})$ and $\Im(W_{ij})$ in Eq. (2). After the introduction of lifted variables $\breve{cs}_{ij}$ and $\breve{sn}_{ij}$ for the cosine and sine functions, respectively, for each branch $(i,j) \in \mathcal{E}$, the non-convex constraints in Eq. (2b) and Eq. (2c) become trilinear term of the form $v_i v_j \breve{cs}_{ij}$ and $v_i v_j \breve{sn}_{ij}$, respectively. This version of the QC relaxation uses the extreme-point representation to obtain the convex envelope of these trilinear terms. It is known in the literature that the extreme-point representation captures the convex hull of a given, single multilinear term [19] and that it is tighter than the recursive McCormick envelopes in Eq. (3c) and (3e) [20], [21]. We also note that the feasible region of this representation is identical to that of the facet characterization of the convex hull of a single trilinear term from [22]. Nevertheless, though we capture the term-wise convex hull, we lose a potential connection between the voltage products in Eq. (2b) and Eq. (2c) that is captured in Model 2 using the shared lifted variable, $\widetilde{v_i v_j}$, to capture $\langle v_i v_j \rangle^M$ in Eq. (3c) and Eq. (3d). Hence, no clear dominance between the original QC relaxation in Model 2 and the QC relaxation using an extreme point representation in the forthcoming Model 3 can be established. This is also depicted in the Venn diagram in Figure 1 and later observed in the computational results as well.

We now define an extreme point before describing the convex envelope. Given a set X, a point $p \in X$ is extreme if there does not exist two other distinct points $p_1, p_2 \in X$ and a non-negative multiplier $\lambda \in [0,1]$ such that $p = \lambda p_1 + (1-\lambda) p_2$. To that end, let $\varphi(x_1, x_2, x_3) = x_1 x_2 x_3$ denote a trilinear term with variable bounds $\boldsymbol{x}_i^{\boldsymbol{l}} \leqslant x_i \leqslant \boldsymbol{x}_i^{\boldsymbol{u}}$ for all $i = 1, 2, 3$. Also, let $\boldsymbol{\xi} = \langle \boldsymbol{\xi_1}, \ldots, \boldsymbol{\xi_8} \rangle$ denote the vector of eight extreme points of $[\boldsymbol{x}_1^{\boldsymbol{l}}, \boldsymbol{x}_1^{\boldsymbol{u}}] \times [\boldsymbol{x}_2^{\boldsymbol{l}}, \boldsymbol{x}_2^{\boldsymbol{u}}] \times [\boldsymbol{x}_3^{\boldsymbol{l}}, \boldsymbol{x}_3^{\boldsymbol{u}}]$ and we use $\boldsymbol{\xi}_{\boldsymbol{k}}^i$ to denote the i^{th} coordinate of $\boldsymbol{\xi_k}$. The extreme points in $\boldsymbol{\xi}$ are given by

$$\boldsymbol{\xi_1} = (\boldsymbol{x}_1^{\boldsymbol{l}}, \boldsymbol{x}_2^{\boldsymbol{l}}, \boldsymbol{x}_3^{\boldsymbol{l}}),\ \boldsymbol{\xi_2} = (\boldsymbol{x}_1^{\boldsymbol{l}}, \boldsymbol{x}_2^{\boldsymbol{l}}, \boldsymbol{x}_3^{\boldsymbol{u}}),\ \boldsymbol{\xi_3} = (\boldsymbol{x}_1^{\boldsymbol{l}}, \boldsymbol{x}_2^{\boldsymbol{u}}, \boldsymbol{x}_3^{\boldsymbol{l}}),$$
$$\boldsymbol{\xi_4} = (\boldsymbol{x}_1^{\boldsymbol{l}}, \boldsymbol{x}_2^{\boldsymbol{u}}, \boldsymbol{x}_3^{\boldsymbol{u}}),\ \boldsymbol{\xi_5} = (\boldsymbol{x}_1^{\boldsymbol{u}}, \boldsymbol{x}_2^{\boldsymbol{l}}, \boldsymbol{x}_3^{\boldsymbol{l}}),\ \boldsymbol{\xi_6} = (\boldsymbol{x}_1^{\boldsymbol{u}}, \boldsymbol{x}_2^{\boldsymbol{l}}, \boldsymbol{x}_3^{\boldsymbol{u}}),$$
$$\boldsymbol{\xi_7} = (\boldsymbol{x}_1^{\boldsymbol{u}}, \boldsymbol{x}_2^{\boldsymbol{u}}, \boldsymbol{x}_3^{\boldsymbol{l}}),\ \text{and}\ \boldsymbol{\xi_8} = (\boldsymbol{x}_1^{\boldsymbol{u}}, \boldsymbol{x}_2^{\boldsymbol{u}}, \boldsymbol{x}_3^{\boldsymbol{u}}). \tag{6}$$

Then, the tightest convex envelope of the trilinear term $x_1 x_2 x_3$ (TRI-CONV) is given by

$$\langle x_1 x_2 x_3 \rangle^\lambda \equiv \begin{cases} \breve{x} = \sum_{k=1}^8 \lambda_k \varphi(\boldsymbol{\xi}_{\boldsymbol{k}}^1, \boldsymbol{\xi}_{\boldsymbol{k}}^2, \boldsymbol{\xi}_{\boldsymbol{k}}^3) \\ x_i = \sum_{k=1}^8 \lambda_k \boldsymbol{\xi}_{\boldsymbol{k}}^i \quad \forall i = 1,2,3 \\ \sum_{k=1}^8 \lambda_k = 1, \quad \lambda_k \geqslant 0 \quad \forall k = 1, \ldots, 8 \end{cases} \tag{7}$$

Notice, that the lifted variable $\breve{x}$ represents the trilinear term i.e., it will replace the right-hand side of Eq. (8b) and (8c). Using the convex envelope for the trilinear term results in the QC relaxation given by Model 3. In Model 3, the constraints defining the lifted variables $\breve{cs}_{ij}$ and $\breve{sn}_{ij}$, for each branch $(i,j) \in \mathcal{E}$, are included in Eq. (8b) and (8c), respectively. We also remark that distinct multiplier variables λ_{ij}^c and λ_{ij}^s are used for capturing the convex envelopes in Eq. (8b) and (8c), respectively.

D. A Strengthened QC Relaxation

This section presents additional constraints to strengthen Model 3. The fundamental idea used to develop these strengthening constraints lies in the observation that different

Model 3 λ-based QC relaxation (QC-LM).

$$\textbf{minimize:} \sum_{i\in\mathcal{G}} \boldsymbol{c}_{2i}(\Re(S_i^g)^2) + \boldsymbol{c}_{1i}\Re(S_i^g) + \boldsymbol{c}_{0i} \tag{8a}$$

subject to: (1b) – (1d), (1g) – (1j), (3b), (3e) – (3f), (5a) – (5b)

$$\Re(W_{ij}) = \langle v_i v_j \breve{cs}_{ij} \rangle^{\lambda^c_{ij}} \quad \forall (i,j) \in \mathcal{E} \tag{8b}$$

$$\Im(W_{ij}) = \langle v_i v_j \breve{sn}_{ij} \rangle^{\lambda^s_{ij}} \quad \forall (i,j) \in \mathcal{E} \tag{8c}$$

sets of multiplier variables λ^c_{ij} and λ^s_{ij} are used for capturing the convex envelopes in Eq. (8b) and (8c), respectively. There are no constraints that link λ^c_{ij} and λ^s_{ij} directly despite sharing two out of three variables in the trilinear term. Adding such a linking constraint intuitively leads to strengthening the relaxation in Model 3. We first state the linking constraint for every branch $(i,j) \in \mathcal{E}$, as follows:

$$\begin{pmatrix} \lambda^c_{ij,1} + \lambda^c_{ij,2} - \lambda^s_{ij,1} - \lambda^s_{ij,2} \\ \lambda^c_{ij,3} + \lambda^c_{ij,4} - \lambda^s_{ij,3} - \lambda^s_{ij,4} \\ \lambda^c_{ij,5} + \lambda^c_{ij,6} - \lambda^s_{ij,5} - \lambda^s_{ij,6} \\ \lambda^c_{ij,7} + \lambda^c_{ij,8} - \lambda^s_{ij,7} - \lambda^s_{ij,8} \end{pmatrix}^T \begin{pmatrix} \boldsymbol{v}_i^{\boldsymbol{l}} \cdot \boldsymbol{v}_j^{\boldsymbol{l}} \\ \boldsymbol{v}_i^{\boldsymbol{l}} \cdot \boldsymbol{v}_j^{\boldsymbol{u}} \\ \boldsymbol{v}_i^{\boldsymbol{u}} \cdot \boldsymbol{v}_j^{\boldsymbol{l}} \\ \boldsymbol{v}_i^{\boldsymbol{u}} \cdot \boldsymbol{v}_j^{\boldsymbol{u}} \end{pmatrix} = 0 \tag{9}$$

This constraint enforces, for each branch $(i,j) \in \mathcal{E}$, the value of the voltage product $v_i v_j$ to take the same value in Eq. (8b) and (8c). The resulting strengthened QC relaxation is summarized in Model 4.

Model 4 Tighter λ-based QC Relaxation (QC-TLM).

$$\textbf{minimize:} \sum_{i\in\mathcal{G}} \boldsymbol{c}_{2i}(\Re(S_i^g)^2) + \boldsymbol{c}_{1i}\Re(S_i^g) + \boldsymbol{c}_{0i} \tag{10a}$$

subject to: (1b) – (1d), (1g) – (1j), (3b), (3e) – (3f), (5a) – (5b), (8b) – (8c), (9)

In the following subsection, we detail the theoretical properties of Model 4 and show that it is tighter than the QC relaxations in Model 2 and 3.

E. Theoretical Properties of the QC-TLM Relaxation

Before presenting the theoretical properties of the strengthened QC relaxation, we first expand constraints in Eq. (1c), (1e), and (1f) for a branch $(i,j) \in \mathcal{E}$ as follows:

$$p_{ij} = \boldsymbol{g}_{ij} v_i^2 - \boldsymbol{g}_{ij} v_i v_j \cos\theta_{ij} - \boldsymbol{b}_{ij} v_i v_j \sin\theta_{ij} \tag{11a}$$

$$q_{ij} = -\boldsymbol{b}_{ij} v_i^2 - \boldsymbol{g}_{ij} v_i v_j \cos\theta_{ij} + \boldsymbol{b}_{ij} v_i v_j \sin\theta_{ij} \tag{11b}$$

After applying the convex envelopes (C-CONV) and (S-CONV) for the cosine and sine terms, respectively, the Eq. (11) reduce to

$$p_{ij} = \boldsymbol{g}_{ij} v_i^2 - \boldsymbol{g}_{ij} v_i v_j \breve{cs}_{ij} - \boldsymbol{b}_{ij} v_i v_j \breve{sn}_{ij} \tag{12a}$$

$$q_{ij} = -\boldsymbol{b}_{ij} v_i^2 - \boldsymbol{g}_{ij} v_i v_j \breve{cs}_{ij} + \boldsymbol{b}_{ij} v_i v_j \breve{sn}_{ij} \tag{12b}$$

Given Eq. (12), the strengthened QC relaxation has the following properties

Theorem 1: The strengthened QC relaxation in Model 4 captures the convex hull of the nonlinear, non-convex term $(-\boldsymbol{g}_{ij} v_i v_j \breve{cs}_{ij} - \boldsymbol{b}_{ij} v_i v_j \breve{sn}_{ij})$ in Eq. (12a).

Proof: See Sec. II-F. ■

Theorem 2: The strengthened QC relaxation in Model 4 captures the convex hull of the nonlinear, non-convex term $(-\boldsymbol{g}_{ij} v_i v_j \breve{cs}_{ij} + \boldsymbol{b}_{ij} v_i v_j \breve{sn}_{ij})$ in Eq. (12b).

Proof: See Sec. II-F. ■

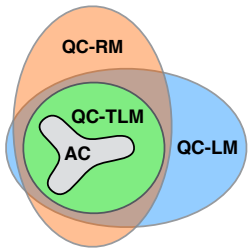

Fig. 1: A Venn diagram representing the feasible sets of QC relaxation with various trilinear term relaxations (set sizes in this illustration are not to scale).

The theoretical properties of the QC relaxations considered here are summarized in Figure 1. To the best of our knowledge, the theoretical results connecting the summation of multilinear terms presented in this paper are new and novel in the global optimization literature. The computational impact of Theorems 1 and 2 are presented in Section IV.

Before, we present the proof of Theorems 1 and 2, we present some results of a computational experiment comparing the three relaxations namely the Recursive-McCormick (RM), the λ-based formulation (LM), and the tightened λ-based formulation (TLM) applied to the sum of two multilinear terms $\phi(x_1,x_2,x_3,x_4) = x_1x_2x_3 + x_1x_2x_4$ defined on $x_i \in [0,1]$ for every $i \in \{1,2,3,4\}$. To that end, we randomly generate 5000 points uniformly in the domain $[0,1]^4$ and for each point $\boldsymbol{x}^k$, calculate the difference between the upper and lower bounds of $\phi(x_1,x_2,x_3,x_4)$ as defined by RM, LM, and TLM formulations. We denote these differences by RMgap($\boldsymbol{x}^k$), LMgap($\boldsymbol{x}^k$), and TLMgap($\boldsymbol{x}^k$), respectively. We then construct two scatter plots, shown in Figure 2, of the points (LMgap($\boldsymbol{x}^k$), RMgap($\boldsymbol{x}^k$)) and (TLMgap($\boldsymbol{x}^k$), RMgap($\boldsymbol{x}^k$)) for all $k = 1,\ldots,5000$, respectively.

The points in scatter plot shown in Fig. 2a, lie above or below the line of unit slope indicating that there are instances where either relaxation i.e., RM or LM, can be stronger than the other. In contrast, all the points in Fig. 2b lie above the line of unit slope indicating that the TLM relaxation is always better than RM. Between LM and TLM relaxations, it is clear from the definition of these relaxations that TLM is stronger than LM. In the next section, we present a proof that TLM indeed captures the convex hull of the sum of trilinear terms with two shared variables.

F. Proof of Theorem 1 and Theorem 2

To keep the proof general, we present it for the sum of trilinear terms $\phi(x_1,x_2,x_3,x_4) = \boldsymbol{\alpha_c} x_1x_2x_3 + \boldsymbol{\alpha_s} x_1x_2x_4$

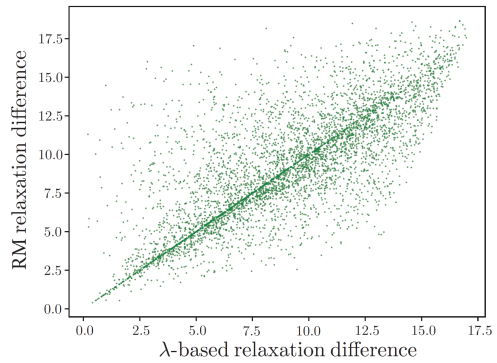

(a) Recursive McCormick (RM) gap vs. LM gap

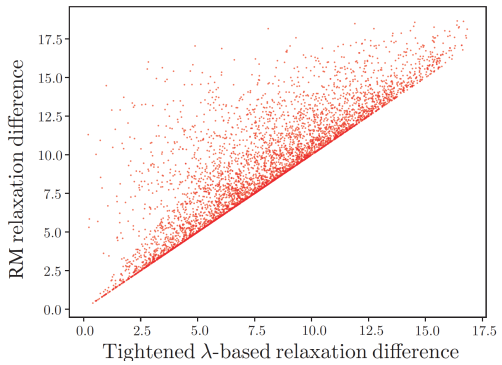

(b) Recursive McCormick (RM) gap vs. TLM gap

Fig. 2: Scatter plots of the gaps obtained using the three relaxations for the sum of trilinear terms $\phi(x_1, x_2, x_3, x_4)$ in the domain $[0, 1]^4$.

where $\boldsymbol{\alpha_c}, \boldsymbol{\alpha_s} \in \mathbb{R}$ and $\boldsymbol{x_i^l} \leqslant x_i \leqslant \boldsymbol{x_i^u}$, $i = 1, .., 4$. Let $K = \{1, \ldots, 16\}$. The convex hull of $z = \phi(x_1, x_2, x_3, x_4)$ is given by

$$\mathcal{S} = \Big\{ z, x_1, .., x_4, \lambda_1, .., \lambda_{16} : z = \sum_{k \in K} \lambda_k \phi(\boldsymbol{\gamma_k}), \sum_{k \in K} \lambda_k = 1, \\ x_i = \sum_{k \in K} \lambda_k \boldsymbol{\gamma_k^i} \ \forall i = 1, .., 4, \ \lambda_k \geqslant 0 \ \forall k \in K \Big\}. \tag{13}$$

Let $\boldsymbol{\gamma^c} = \langle \boldsymbol{\gamma_1^c}, \ldots, \boldsymbol{\gamma_8^c} \rangle$ and $\boldsymbol{\gamma^s} = \langle \boldsymbol{\gamma_1^s}, \ldots, \boldsymbol{\gamma_1^s} \rangle$ and $\boldsymbol{\gamma} = \langle \boldsymbol{\gamma_1}, \ldots, \boldsymbol{\gamma_{16}} \rangle$ denote the extreme points of $[\boldsymbol{x_1^l}, \boldsymbol{x_1^u}] \times [\boldsymbol{x_2^l}, \boldsymbol{x_2^u}] \times [\boldsymbol{x_3^l}, \boldsymbol{x_3^u}]$ and $[\boldsymbol{x_1^l}, \boldsymbol{x_1^u}] \times [\boldsymbol{x_2^l}, \boldsymbol{x_2^u}] \times [\boldsymbol{x_4^l}, \boldsymbol{x_4^u}]$, and $[\boldsymbol{x_1^l}, \boldsymbol{x_1^u}] \times [\boldsymbol{x_2^l}, \boldsymbol{x_2^u}] \times [\boldsymbol{x_3^l}, \boldsymbol{x_3^u}] \times [\boldsymbol{x_4^l}, \boldsymbol{x_4^u}]$, respectively. The extreme points in $\boldsymbol{\gamma^c}$, $\boldsymbol{\gamma^s}$ and $\boldsymbol{\gamma}$ are ordered similar to the extreme points in Eq. (6), i.e., in dictionary order. The strengthened QC relaxation represents the term $z = \phi(x_1, x_2, x_3, x_4)$ by using the following equations:

$$\mathcal{S}_{QC} = \Big\{ z, z_c, z_s, x_1, .., x_4, \lambda_1^c, .., \lambda_8^c, \lambda_1^s, .., \lambda_8^s : \\ z_c = \langle x_1 x_2 x_3 \rangle^{\lambda^c}, \quad z_s = \langle x_1 x_2 x_4 \rangle^{\lambda^s}, \\ z = \boldsymbol{\alpha_c} z_c + \boldsymbol{\alpha_s} z_s, \ \text{Eq. (9) with } x_1 \equiv v_i, \ x_2 \equiv v_j \Big\}. \tag{14}$$

We show that the projection of (14), $\mathcal{P}(\mathcal{S}_{QC})$, on to the (z, x_1, x_2, x_3, x_4) space is identical to its convex hull given in (13). First, we set

$$\lambda_1^c = \lambda_1 + \lambda_2 \qquad \lambda_1^s = \lambda_1 + \lambda_3 \tag{15a}$$
$$\lambda_2^c = \lambda_3 + \lambda_4 \qquad \lambda_2^s = \lambda_2 + \lambda_4 \tag{15b}$$
$$\lambda_3^c = \lambda_5 + \lambda_6 \qquad \lambda_3^s = \lambda_5 + \lambda_7 \tag{15c}$$
$$\lambda_4^c = \lambda_7 + \lambda_8 \qquad \lambda_4^s = \lambda_6 + \lambda_8 \tag{15d}$$
$$\lambda_5^c = \lambda_9 + \lambda_{10} \qquad \lambda_5^s = \lambda_9 + \lambda_{11} \tag{15e}$$
$$\lambda_6^c = \lambda_{11} + \lambda_{12} \qquad \lambda_6^s = \lambda_{10} + \lambda_{12} \tag{15f}$$
$$\lambda_7^c = \lambda_{13} + \lambda_{14} \qquad \lambda_7^s = \lambda_{13} + \lambda_{15} \tag{15g}$$
$$\lambda_8^c = \lambda_{15} + \lambda_{16} \qquad \lambda_8^s = \lambda_{14} + \lambda_{16}. \tag{15h}$$

With the above assignment, it is easy to check that $\lambda_i^c, \lambda_i^s \geqslant 0$, $\sum_i \lambda_i^c = \sum_i \lambda_i^s = 1$ and $\boldsymbol{\alpha_c} \sum_i \lambda_i^c \gamma_i^c + \boldsymbol{\alpha_s} \sum_i \lambda_i^s \gamma_i^s = \sum_i \lambda_i \gamma_i$. This shows that $(z, x_1, x_2, x_3, x_4) \in \mathcal{P}(\mathcal{S}_{QC})$ and hence that $\mathcal{S} \subseteq \mathcal{P}(\mathcal{S}_{QC})$.

Let $(\lambda_{odd}^c, \lambda_{odd}^s)$ and $(\lambda_{even}^c, \lambda_{even}^s)$ represent (λ^c, λ^s) multipliers with odd ($\{1, 3, 5, 7\}$) and even ($\{2, 4, 6, 8\}$) indices, respectively. Let

$$\lambda_{1|4} = \lambda_{\text{odd}}^s - \lambda_{\text{even}}^c + \max\{\lambda_{\text{even}}^c - \lambda_{\text{odd}}^s, 0\} \tag{16a}$$
$$\lambda_{2|4} = \lambda_{\text{even}}^s - \max\{\lambda_{\text{even}}^c - \lambda_{\text{odd}}^s, 0\} \tag{16b}$$
$$\lambda_{3|4} = \lambda_{\text{even}}^c - \max\{\lambda_{\text{even}}^c - \lambda_{\text{odd}}^s, 0\} \tag{16c}$$
$$\lambda_{4|4} = 0 + \max\{\lambda_{\text{even}}^c - \lambda_{\text{odd}}^s, 0\} \tag{16d}$$

where, $\lambda_{i|4} = (\lambda_i, \lambda_{i+4}, \lambda_{i+8}, \lambda_{i+12})$. By construction, the above assignment of λ satisfies the system of equations in (15). As a result, we have $\boldsymbol{\alpha_c} \sum_i \lambda_i^c \gamma_i^c + \boldsymbol{\alpha_s} \sum_i \lambda_i^s \gamma_i^s = \sum_i \lambda_i \gamma_i$. Further, $\sum_i \lambda_i = \sum_i \lambda_i^s = 1$. What is left is to show that $\lambda_i \geqslant 0 \ \forall i$. We can rewrite (16) as

$$\lambda_{1|4} = \max\{\lambda_{\text{odd}}^s - \lambda_{\text{even}}^c, 0\} \tag{17a}$$
$$\lambda_{2|4} = \min\{\lambda_{\text{even}}^s + \lambda_{\text{odd}}^s - \lambda_{\text{even}}^c, \lambda_{\text{even}}^s\} \tag{17b}$$
$$\lambda_{3|4} = \min\{\lambda_{\text{odd}}^s, \lambda_{\text{even}}^c\} \tag{17c}$$
$$\lambda_{4|4} = \max\{\lambda_{\text{even}}^c - \lambda_{\text{odd}}^s, 0\}. \tag{17d}$$

We observe that the expressions on the RHS of Equations (17a),(17c) and (17d) are non-negative. To show that $\lambda_{2|4}$ in (17b) is also non-negative, we need the following additional result.

Lemma 3: The multipliers λ^c and λ^s satisfy

$$\lambda_{\text{even}}^c + \lambda_{\text{odd}}^c = \lambda_{\text{even}}^s + \lambda_{\text{odd}}^s. \tag{18}$$

Using Lemma 3, we see that $\lambda_{\text{even}}^s + \lambda_{\text{odd}}^s - \lambda_{\text{even}}^c = \lambda_{\text{odd}}^c$, and thus $\lambda_{2|4} = \min\{\lambda_{\text{odd}}^c, \lambda_{\text{even}}^s\} \geqslant 0$, and hence that $\mathcal{P}(\mathcal{S}_{QC}) \subseteq \mathcal{S}$. With this, proof of the theorem is complete.

1) Proof of Lemma 3: Using Eq (7) and the coupling constraint in (9), we conclude that λ^c, λ^s satisfy the following constraint.

$$\begin{pmatrix} \boldsymbol{x_1^l} & \boldsymbol{x_2^l} & \boldsymbol{x_1^l x_2^l} \\ \boldsymbol{x_1^l} & \boldsymbol{x_2^u} & \boldsymbol{x_1^l x_2^u} \\ \boldsymbol{x_1^u} & \boldsymbol{x_2^l} & \boldsymbol{x_1^u x_2^l} \\ \boldsymbol{x_1^u} & \boldsymbol{x_2^u} & \boldsymbol{x_1^u x_2^u} \end{pmatrix} \left(\lambda_{\text{odd}}^c + \lambda_{\text{even}}^c - \lambda_{\text{odd}}^s - \lambda_{\text{even}}^s\right) = 0. \tag{19}$$

Since the four extreme points in the rows of the matrix in LHS of (19) are assumed to be distinct, the matrix is full rank (3) and we must have $\lambda_{\text{odd}}^c + \lambda_{\text{even}}^c - \lambda_{\text{odd}}^s - \lambda_{\text{even}}^s = 0$.

III. Optimization-Based Bound Tightening

We now present an Optimization-Based Bound Tightening (OBBT) algorithm that can be applied to any convex relaxation of the AC-OPF problem with voltage magnitude and phase angle difference variables and is aimed at tightening the bounds on these variables. It has been observed in [10], [14] that the SDP and QC relaxations of AC-OPF benefit substantially with tight variable bounds. The algorithm proceeds as follows: Let Ω denote the feasible set of any one of the QC relaxations of the AC-OPF problem presented in this paper. Then, two optimization problems, one for each variable in the set $\mathcal{V} = \{v_i \, \forall i \in \mathcal{N}, \theta_{ij} \, \forall (i,j) \in \mathcal{E}\}$ are solved to find the maximum and minimum value of the variable subject to the constraints in Ω. Observe that each optimization problem is convex and upon computing tighter variable bounds for each variable in the set $\mathcal{V}$, a new, tighter QC relaxation is constructed, if any bound has changed. This process is repeated until a fixed point is reached, i.e., none of the variable bounds change between subsequent iterations. A pseudo-code of this procedure is given in Algorithm 1.

Algorithm 1 The OBBT Algorithm

Input: A QC Relaxation (Model 2/3/4) to construct Ω
Output: $\boldsymbol{v^l}$, $\boldsymbol{v^u}$, $\boldsymbol{\theta^l}$, $\boldsymbol{\theta^u}$

repeat
  $\boldsymbol{v^{l0}}, \boldsymbol{v^{u0}}, \boldsymbol{\theta^{l0}}, \boldsymbol{\theta^{u0}} \leftarrow \boldsymbol{v^l}, \boldsymbol{v^u}, \boldsymbol{\theta^l}, \boldsymbol{\theta^u}$
  $\Omega \leftarrow$ QC relaxation given $\boldsymbol{v^{l0}}, \boldsymbol{v^{u0}}, \boldsymbol{\theta^{l0}}, \boldsymbol{\theta^{u0}}$
  for all $i \in \mathcal{N}$ **do**
    $\boldsymbol{v_i^l} \leftarrow \min\{v_i : \Omega\}$
    $\boldsymbol{v_i^u} \leftarrow \max\{v_i : \Omega\}$
  for all $(i,j) \in \mathcal{E}$ **do**
    $\boldsymbol{\theta_{ij}^l} \leftarrow \min\{\theta_{ij} : \Omega\}$
    $\boldsymbol{\theta_{ij}^u} \leftarrow \max\{\theta_{ij} : \Omega\}$
until $\boldsymbol{v^{l0}}, \boldsymbol{v^{u0}}, \boldsymbol{\theta^{l0}}, \boldsymbol{\theta^{u0}} = \boldsymbol{v^l}, \boldsymbol{v^u}, \boldsymbol{\theta^l}, \boldsymbol{\theta^u}$

A. OBBT for Global Optimization

The value of using the OBBT algorithm for characterizing the AC-OPF feasibility set was originally highlighted in [10]. However, if the primary goal is to improve the objective lower bound of the AC-OPF problem, then adding the following additional, convex, upper bound constraint to Ω can vastly improve the algorithm:

$$\sum_{i \in \mathcal{G}} \boldsymbol{c_{2i}} (\Re(S_i^g)^2) + \boldsymbol{c_{1i}} \Re(S_i^g) + \boldsymbol{c_{0i}} \leqslant f^* \qquad (20)$$

where, f^* denotes the cost of any feasible AC-OPF solution or in particular, a local optimal AC-OPF solution. This additional constraint provides a significant advantage in reducing the search space for each convex optimization problem solved during the OBBT algorithm and is routinely used in the global optimization literature [12], [23], [24]. We refer to the version of Algorithm 1 that includes constraint (20) as GO-OBBT.

IV. Numerical Results

This section highlights the computational differences of the proposed QC relaxations (i.e. QC-RM, QC-LM, and QC-TLM) via two detailed numerical studies. The first study revisits the OBBT algorithm from [10] and demonstrates that QC-TLM provides tighter voltage magnitudes and voltage angle bounds with a negligible change in runtime. The second study explores the effectiveness of the QC relaxations for providing lower bounds on the AC-OPF both with and without bound tightening.

A. Test Cases and Computational Setting

This study focuses on 57 networks from the IEEE PES PGLib AC-OPF v18.08 benchmark library [25], which are all under 1000 buses. All of QC relaxations and the OBBT algorithms were implemented in Julia v0.6 using the optimization modeling layer JuMP.jl v0.18 [26]. All of the implementations are available as part of the open-source package PowerModels.jl v0.8, a Julia/JuMP package for power network optimization [27]. Individual non-convex AC-OPF problems and convex QC-OPF relaxations were solved with Ipopt [28] using the HSL-MA27 linear algebra solver. The convex relaxations in the OBBT algorithms were solved with Gurobi v8.0 [29] for improved performance and numerical accuracy. All solvers were set to optimality tolerance of 10^{-6} and the OBBT algorithm was configured with a minimum bound width and an average improvement tolerance [27] of 10^{-4}. Finally, all of the algorithms were evaluated on HPE ProLiant XL170r servers with two Intel 2.10 GHz CPUs and 128 GB of memory.

B. OBBT runtimes

Figure 3 presents the distribution of OBBT runtimes for the various QC relaxations presented in this paper, both in terms of total runtime and an ideal parallel runtime. These results highlight that there is no significant difference in the runtime of the QC relaxations considered here. It is also noteworthy to mention that although the proposed strengthened QC relaxation introduces $2^4(|\mathcal{E}|)$ additional λ variables into the optimization problem, the runtimes remain the same possibly due to the reduction in the size of the feasible region captured by the convex hull relaxations.

C. Computing AC-OPF Lower Bounds

Table I presents AC-OPF optimality gaps provided by the proposed QC relaxations both with and without bound tightening, where the percentage gap is defined as $100 * (ACHeuristic - Relaxation)/ACHeuristic$. For each network considered, the table reports: (1) The AC objective value from solving the non-convex problem with Ipopt; (2) the optimally gap of each relaxation, without bound tightening; (3) the optimally gap of each relaxation after running GO-OBBT. In the interest of brevity, cases where the base QC-RM gap is $< 1.0\%$ are omitted. Bold text is used to highlight the best result in each row of the table.

Again, the results in Table I highlight the theoretical result showing that the QC-TLM relaxation dominates both

TABLE I: The Quality of QC Relaxations for AC-OPF Lower Bounds.

Case	$\|N\|$	$\|E\|$	AC Obj.	Base Opt. Gap (%)			GO-OBBT Opt. Gap (%)		
				RM	LM	TLM	RM	LM	TLM
Typical Operating Conditions (TYP)									
case3_lmbd	3	3	5.8126e+03	1.22	**0.97**	**0.97**	0.01	0.01	0.01
case5_pjm	5	6	1.7552e+04	14.55	14.55	14.55	6.01	6.14	**5.80**
case30_ieee	30	41	1.1974e+04	10.78	**10.67**	**10.67**	0.01	0.01	0.01
case118_ieee	118	186	1.1580e+05	2.20	**2.18**	**2.18**	0.02	0.02	0.02
case162_ieee_dtc	162	284	1.2615e+05	7.54	7.54	7.54	0.05	**0.03**	0.04
case240_pserc	240	448	3.5700e+06	3.81	3.80	**3.79**	2.37	2.36	**2.30**
case300_ieee	300	411	6.6422e+05	2.56	**2.54**	**2.54**	**0.06**	**0.06**	0.07
case500_tamu	500	597	7.2578e+04	5.39	5.39	5.39	0.01	0.01	0.01
case588_sdet	588	686	3.8155e+05	1.68	1.68	1.68	0.33	0.35	**0.30**
Congested Operating Conditions (API)									
case3_lmbd_api	3	3	1.1242e+04	5.63	4.58	**4.56**	0.04	0.04	0.04
case5_pjm_api	5	6	7.6377e+04	4.09	4.09	4.09	0.01	0.01	0.01
case14_ieee_api	14	20	1.3311e+04	1.77	1.77	1.77	0.02	**0.01**	0.02
case24_ieee_rts_api	24	38	1.3495e+05	13.01	11.06	**11.01**	0.04	0.04	0.04
case30_as_api	30	41	4.9962e+03	44.61	44.61	44.61	**0.72**	0.77	0.80
case30_fsr_api	30	41	7.0115e+02	2.76	2.76	2.76	0.13	0.13	0.13
case30_ieee_api	30	41	2.4032e+04	3.73	3.73	3.73	0.04	0.04	0.04
case39_epri_api	39	46	2.5721e+05	1.57	1.57	1.57	0.02	0.02	0.02
case73_ieee_rts_api	73	120	4.2273e+05	11.07	9.56	**9.51**	**0.41**	**0.41**	0.46
case89_pegase_api	89	210	1.4198e+05	8.13	8.13	8.13	1.69	1.50	**1.31**
case118_ieee_api	118	186	3.1642e+05	28.63	28.62	**28.51**	4.27	3.64	**3.32**
case162_ieee_dtc_api	162	284	1.4351e+05	5.44	5.44	5.44	**0.06**	**0.06**	0.07
case179_goc_api	179	263	2.1326e+06	7.18	7.21	**7.10**	0.03	**0.02**	**0.02**
Small Angle Difference Conditions (SAD)									
case3_lmbd_sad	3	3	5.9593e+03	1.42	**1.38**	**1.38**	0.03	0.03	0.03
case14_ieee_sad	14	20	6.7834e+03	7.16	6.38	**6.32**	0.30	0.30	0.30
case24_ieee_rts_sad	24	38	7.6943e+04	2.93	2.77	**2.74**	0.23	0.23	0.23
case30_as_sad	30	41	8.9749e+02	2.32	2.32	**2.31**	**0.31**	0.32	0.32
case30_ieee_sad	30	41	1.1974e+04	3.42	3.28	**3.24**	0.01	0.01	0.01
case73_ieee_rts_sad	73	120	2.2775e+05	2.54	2.39	**2.38**	**0.09**	**0.09**	0.10
case118_ieee_sad	118	186	1.2924e+05	9.48	9.31	**9.30**	**0.24**	0.25	0.26
case162_ieee_dtc_sad	162	284	1.2704e+05	8.02	7.98	**7.97**	0.08	0.08	0.08
case179_goc_sad	179	263	8.3560e+05	1.05	**1.04**	**1.04**	0.02	0.02	0.02
case240_pserc_sad	240	448	3.6565e+06	5.24	5.22	**5.21**	2.83	2.82	**2.70**
case300_ieee_sad	300	411	6.6431e+05	2.36	2.30	**2.29**	0.04	0.04	0.04
case500_tamu_sad	500	597	7.9234e+04	7.90	7.90	7.90	0.31	0.34	**0.30**
case588_sdet_sad	588	686	4.0427e+05	6.26	6.28	**6.21**	0.25	0.26	**0.24**

the QC-RM and QC-LM relaxations. It also highlights two interesting points: (1) In some cases the QC-TLM relaxation can provide benefits without bound tightening, e.g. case24_ieee_rts_api, case73_ieee_rts_api and case14_ieee_sad; (2) the QC-TLM relaxation's most significant benefits occur in the most challenging GO-OBBT cases, e.g. case89_peg ase_api, case118_ieee_api. It is important to note that small discrepancies in the GO-OBBT optimality gaps are observed. These are due to numerical challenges resulting from the finite precision of floating point arithmetic and only occur in cases where the optimality gap is close to zero.

V. Conclusions

In summary, this paper presents a novel strengthened version of the QC relaxation and shows its theoretical tightness and its effectiveness in computing better variable bounds and reducing the optimality gap on a wide range of test networks, when used in conjunction with bound-tightening techniques. For numerous benchmark instances, the proposed QC relaxation provides non-trivial improvements in the optimality gaps, both in the base relaxation and also when applied in conjunction with the OBBT algorithm for obtaining near global optimum solutions.

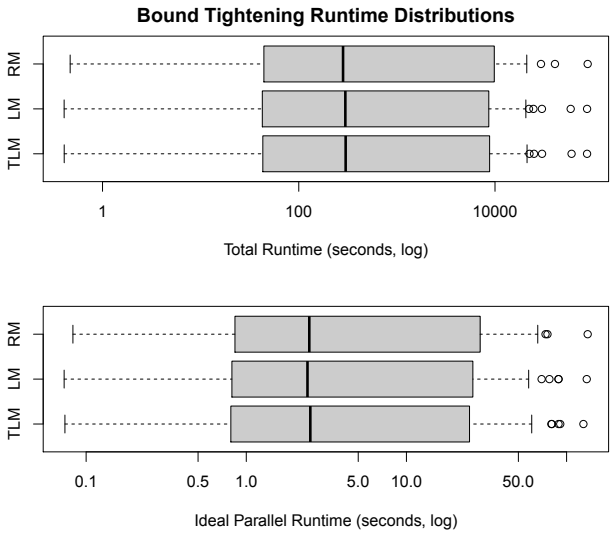

Fig. 3: Runtime distributions of OBBT with various QC relaxations. The lower and upper ends of the boxes reflect the first and third quanrtiles, the lines inside the boxes denote the median, and the circles are outliers.

Future work: Although the gap improvements for a few instances may not seem very significant in Table I, *the proposed convex relaxations are fundamental in nature and can be applied to other useful variants of the AC-OPF relaxations in the literature, such as in the inclusion of cycle-based constraints* [3]. For example, for any 3-cycle $(i-j-k)$ in a network, the equality $\theta_{ij} + \theta_{jk} - \theta_{ik} = 0$, leads to the following constraints in the $\breve{cs}$-$\breve{sn}$ space of variables by applying to this equation, cos and sin, respectively:

$$\breve{cs}_{ij}\breve{cs}_{jk}\breve{cs}_{ik} + \breve{cs}_{ij}\breve{sn}_{jk}\breve{sn}_{ik} - \breve{sn}_{ij}\breve{sn}_{jk}\breve{cs}_{ik} + \breve{sn}_{ij}\breve{cs}_{jk}\breve{sn}_{ik} = 1,$$
$$\breve{sn}_{ij}\breve{cs}_{jk}\breve{cs}_{ik} + \breve{sn}_{ij}\breve{sn}_{jk}\breve{sn}_{ik} + \breve{cs}_{ij}\breve{sn}_{jk}\breve{cs}_{ik} - \breve{cs}_{ij}\breve{cs}_{jk}\breve{sn}_{ik} = 0.$$

It can be observed that the proposed extreme-point convex hull relaxations with strengthened linking constraints can be applied on shared bilinear terms such as $\breve{cs}_{ij}\breve{cs}_{jk}$, $\breve{cs}_{ij}\breve{sn}_{ik}$, etc. Thus, future work includes extensions to account for cycle-induced relaxations in the AC-OPF problem.

REFERENCES

[1] J. Carpentier, "Contribution a l'etude du dispatching economique," *Bulletin de la Societe Francaise des Electriciens*, vol. 3, no. 1, pp. 431–447, 1962.

[2] S. Frank, I. Steponavice, and S. Rebennack, "Optimal power flow: a bibliographic survey ii," *Energy Systems*, vol. 3, no. 3, pp. 259–289, 2012.

[3] B. Kocuk, "Global optimization methods for optimal power flow and transmission switching problems in electric power systems," Ph.D. dissertation, Georgia Institute of Technology, 2016.

[4] M. Lu, H. Nagarajan, R. Bent, S. Eksioglu, and S. Mason, "Tight piecewise convex relaxations for global optimization of optimal power flow," in *Power Systems Computation Conference*. IEEE, 2018, pp. 1–7.

[5] K. Lehmann, A. Grastien, and P. Van Hentenryck, "AC-feasibility on tree networks is NP-hard," *IEEE Transactions on Power Systems*, vol. 31, no. 1, pp. 798–801, 2016.

[6] X. Bai, H. Wei, K. Fujisawa, and Y. Wang, "Semidefinite programming for optimal power flow problems," *International Journal of Electrical Power & Energy Systems*, vol. 30, no. 6-7, pp. 383–392, 2008.

[7] R. A. Jabr, "Radial distribution load flow using conic programming," *IEEE trans. on power systems*, vol. 21, no. 3, pp. 1458–1459, 2006.

[8] H. Hijazi, C. Coffrin, and P. V. Hentenryck, "Convex quadratic relaxations for mixed-integer nonlinear programs in power systems," *Math. Programming Computation*, vol. 9, no. 3, pp. 321–367, Sep 2017.

[9] D. K. Molzahn and I. A. Hiskens, "Moment-based relaxation of the optimal power flow problem," in *Power Systems Computation Conference (PSCC), 2014*. IEEE, 2014, pp. 1–7.

[10] C. Coffrin, H. L. Hijazi, and P. Van Hentenryck, "Strengthening convex relaxations with bound tightening for power network optimization," in *International Conference on Principles and Practice of Constraint Programming*. Springer, 2015, pp. 39–57.

[11] C. Coffrin and L. Roald, "Convex relaxations in power system optimization: A brief introduction," *arXiv preprint:1807.07227*, 2018.

[12] H. Nagarajan, M. Lu, S. Wang, R. Bent, and K. Sundar, "An adaptive, multivariate partitioning algorithm for global optimization of nonconvex programs," *Journal of Global Optimization*, vol. 74, pp. 639–675, 2019.

[13] Y. Puranik and N. V. Sahinidis, "Bounds tightening based on optimality conditions for nonconvex box-constrained optimization," *Journal of Global Optimization*, vol. 67, no. 1-2, pp. 59–77, 2017.

[14] C. Chen, A. Atamtürk, and S. S. Oren, "Bound tightening for the alternating current optimal power flow problem," *IEEE Trans. Power Syst.*, vol. 31, no. 5, pp. 3729–3736, 2016.

[15] D. Bienstock and A. Verma, "Strong NP-hardness of AC power flows feasibility," *arXiv preprint:1512.07315*, 2015.

[16] C. Coffrin, H. L. Hijazi, and P. V. Hentenryck, "The QC Relaxation: A Theoretical and Computational Study on Optimal Power Flow," *IEEE Trans. on Power Systems*, vol. 31, no. 4, pp. 3008–3018, July 2016.

[17] G. P. McCormick, "Computability of global solutions to factorable nonconvex programs: Part i—convex underestimating problems," *Mathematical programming*, vol. 10, no. 1, pp. 147–175, 1976.

[18] C. Coffrin, H. L. Hijazi, and P. V. Hentenryck, "Strengthening the SDP relaxation of AC power flows with convex envelopes, bound tightening, and valid inequalities," *IEEE Transactions on Power Systems*, vol. 32, no. 5, pp. 3549–3558, Sept 2017.

[19] A. D. Rikun, "A convex envelope formula for multilinear functions," *Journal of Global Optimization*, vol. 10, no. 4, pp. 425–437, 1997.

[20] M. R. Narimani, D. K. Molzahn, H. Nagarajan, and M. L. Crow, "Comparison of Various Trilinear Monomial Envelopes for Convex Relaxations of Optimal Power Flow Problems," in *IEEE Global Conference on Signal and Information Processing*. IEEE, 2018.

[21] H. Nagarajan, K. Sundar, H. Hijazi, and R. Bent, "Convex hull formulations for mixed-integer multilinear functions," in *Proceedings of the XIV International Global Optimization Workshop (LEGO 18)*, 2018.

[22] C. A. Meyer and C. A. Floudas, "Trilinear monomials with mixed sign domains: Facets of the convex and concave envelopes," *Journal of Global Optimization*, vol. 29, no. 2, pp. 125–155, 2004.

[23] J. Liu, A. Castillo, J.-P. Watson, and C. D. Laird, "Global solution strategies for the network-constrained unit commitment problem with ac transmission constraints."

[24] H. Nagarajan, M. Lu, E. Yamangil, and R. Bent, "Tightening McCormick relaxations for nonlinear programs via dynamic multivariate partitioning," in *International Conference on Principles and Practice of Constraint Programming*. Springer, 2016, pp. 369–387.

[25] The IEEE PES Task Force on Benchmarks for Validation of Emerging Power System Algorithms, "PGLib Optimal Power Flow Benchmarks," Published online at https://github.com/power-grid-lib/pglib-opf, accessed: August 10, 2018.

[26] I. Dunning, J. Huchette, and M. Lubin, "JuMP: A modeling language for mathematical optimization," *SIAM Review*, vol. 59, no. 2, pp. 295–320, 2017.

[27] C. Coffrin, R. Bent, K. Sundar, Y. Ng, and M. Lubin, "PowerModels.jl: An open-source framework for exploring power flow formulations," in *2018 Power Systems Computation Conference*, June 2018, pp. 1–8.

[28] A. Wächter and L. T. Biegler, "On the implementation of a primal-dual interior point filter line search algorithm for large-scale nonlinear programming," *Math. Prog.*, vol. 106, no. 1, pp. 25–57, 2006.

[29] Gurobi, "Gurobi optimizer reference manual," 2018. [Online]. Available: http://www.gurobi.com